15th Triennial World Congress, Barcelona, Spain

ENHANCED PATH PLANNING FOR ARTICULATED AND SKID STEERING MINING VEHICLES

Vladimir Polotski

NSERC Industrial Chair in Mining Automation, Ecole Polytechnique de Montreal
Phone 514 340-4711 ext 4175, FAX (514) 340-5802 email: *polotski@ai.polymtl.ca*

Abstract: Autonomous guidance of the mining vehicle is based on the path tracking algorithm that use pre-calculated desired paths. These paths are often calculated without taking into account the nonholonomic nature of the vehicle motion. As a result the calculated path might be not feasible and the path tracking controller will be required to correct the situation, deteriorating at the same time the overall performance of the guiding algorithm. In this paper we describe path-planning algorithms for articulated and skid steering vehicles used in mining applications. We propose numerically stable procedure for computing off-line the skidding and articulation angles. The results of these computations complement the conventional path-planing procedures and improve significantly the path-tracking precision, and overall guidance performance. *Copyright ©2002 IFAC*

Keywords: numerical stability, autonomous guidance, path-planning.

1. INTRODUCTION

The hazardous environment of a mine demands an increasing degree of autonomy of the mobile mining equipment in order to keep the human presence on the site minimal. This research targets autonomous guidance of slow moving heavy underground and surface mining machines as Laud-Haul-Dumping machines (LHD) and blast-hole drills.

An underground LHD, equipped with a bucket, has to move back and forth along the narrow drifts between loading and dumping sites where it stops for executing loading/dumping ore. A surface drill, equipped with a very tall drilling rig and two actuated tracks, has to move slowly between predefined locations where it stops for drilling holes that are subsequently filled with explosives.

Developing autonomously guided LHD's and drills will allow the remote supervised control of the machine and might evolve to the multi-unit supervision by a single remote operator, resulting in higher efficiency, and greater safety.

Some degree of autonomy is achieved in the control of underground machines. Much more has to be done in surface machine automation. However, in both cases there are still many challenges in transferring the advanced results obtained from planning and control of autonomous robots to industrial implementations. Some recent steps towards converting real mining machines to autonomous units with on-board navigation and path following capabilities are described in (DeSantis, 1997; Polotski *et al.*, 2000) for underground mining and (Peck and Hendrics, 1997; Ahmadi *et al.*, 2000) for open pit mining.

The vehicle guidance problem is conventionally devised into the path-planning and path-tracking phase. First phase is mostly addressed on theoretical level. second phase is widely analyzed from practical point of view, however the path to be followed is most often taken in a simplified form as a set of the straight segments and circular arcs. This approach being acceptable from the geometrical point of view neglects the computation of some parameters useful for control algorithms, thus letting to the path tracking controllers to correct the situation.

This work demonstrates how the off-line computation of

additional parameters such as articulation angle for articulated vehicles and skidding angle for skid-steering vehicles may improve the overall performance of the vehicle guidance without increasing the complexity and the cost of the system. The paper is organized as follows. Section 2 and 3 are devoted to articulated vehicles. A path-tracking control for articulated vehicles has been the subject of numerous works (DeSantis, 1997; l. Bushnell *et al.*, 1994; Polotski, 2000) We analyze here the path planning computations that must precede the path-tracking, but have not received substantial attention of the researchers. We calculate the articulation angle and demonstrate that for backward maneuver our algorithm gives the correct result despite the numerical instability that deteriorate conventional computations. In section 4 and 5 we study skid steering vehicles. A path-tracking controller for this type of vehicles has been recently proposed in (Ahmadi *et al.*, 2000). We extend the planning procedure and obtain, more accurately, the vehicle heading. Taking into account the shape of the path and the required vehicle speed, we calculate the corresponding lateral slippage, and deduce the slip-angle and vehicle heading for subsequent use in path-tracking controller.

2. MODELING OF AN ARTICULATED VEHICLE

A two-part four-wheel vehicle articulated in the middle is under consideration. The steering action is performed by changing articulation angle.

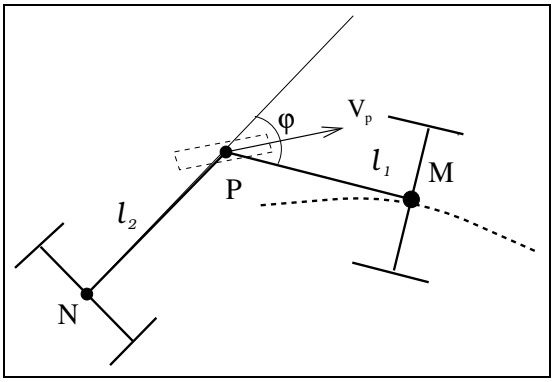

Figure 1: *Scheme of articulated vehicle*

Let M and N be the middle points of two axles with the junction point P (see Figure 1). Let $\overline{V}_M$, $\overline{V}_N$, and $\overline{V}_P$ be the velocities of points M, N, P respectively. The sign of V_M is positive if $\overline{V}_M \uparrow\uparrow \overline{PM}$ and negative otherwise. Let denote by φ the articulation angle between $\overline{PM}$ and $\overline{NP}$ (positive for anti-clockwise case). Let us mark a point M as "front point". Let X, Y, ψ be Cartesian its coordinates and heading angle of $\overline{PM}$ with respect to the world coordinates, and let denote by δ the angle of velocity vector V_P at point P with the front part $\overline{PM}$ of the vehicle. We will consider this angle as the *generalized control input*.

For low speed vehicles like those usually met in mining applications the kinematics level of description seems to be appropriate. The kinematic equations have the following form (PM and NP are denoted by l_1 and l_2 respectively):

$$\frac{dX}{dt} = V_M \cos\psi \tag{1}$$

$$\frac{dY}{dt} = V_M \sin\psi \tag{2}$$

$$\frac{d\psi}{dt} = -V_M \tan\delta/l_1 \tag{3}$$

$$\frac{d\varphi}{dt} = V_M\,(-\frac{\sin\varphi}{l_2} + \tan\delta(\frac{1}{l_1} + \frac{\cos\varphi}{l_2}) \tag{4}$$

The term "*generalized input*" means that this model may describe both actuated articulation and tractor-trailer scheme. If only one part of the vehicle is steered the model describes the motion of a car with trailer (both forward and backward cases). One can see that equations (1)–(3) describe the unicycle motion and equation (4) corresponds to the "internal degree of freedom". Another approach based on the new reference point serving as linearizing or flattening point is discussed in (Polotski, 2000)

3. ARTICULATION PLANNING

A smooth trajectory of the point M directly specifies the trajectory of the point P as another point of the same rigid body (tricycles PM). We will first study the behavior of the tricycle NP with respect to the first one. Let us denote the *generalized input* $\tan\delta$ by p and introduce the length s(t) along the path of point M and an angular variable $\alpha = s(t)/l_2$. We have $d\alpha = ds/l_2 = |V_M|\,dt/l_2$

Changing the variable in (4) from t to α and using notation $\varepsilon = (l_2 - l_1)/(2l_1)$ we obtain

$$\frac{d\varphi}{d\alpha} = \text{sign}(V_M)(-\sin\varphi + p(\alpha)(\cos\varphi + 1 + 2\varepsilon)) \tag{5}$$

This equation has the type studied in (Kamke, 19833) (Eq. 1.79). and is equivalent to the Riccati equation. Changing variable from φ to $u = \tan(\varphi/2)$ we get

$$\frac{du}{d\alpha} = \text{sign}(V_M)\,(-u + p(\alpha)(1+\varepsilon) - p(\alpha)\varepsilon U^2) \tag{6}$$

The factor sign(V_M) is positive for forward motion and negative otherwise. The right-hand side of (5),change the sign with this factor becoming the stable for forward motion and unstable otherwise Let us first discuss the case $\varepsilon = 0$ that corresponds to the symmetrical machine $l_1 = l_2$. Riccati equation 5 is reduced in this case to the linear one:

$$\frac{du}{d\alpha} = \text{sign}(V_M)(-u + p(\alpha)) \tag{7}$$

This equation has unique exponentially stable "attractive" solution for forward motion and an unstable one otherwise. For backward motion, the growing solutions (see Figure 2, right bottom plot) escape from one "repulsive" solution and converge to the singular solution $\varphi = \pi$ of (5). These solutions do not correspond to any feasible motion of the vehicle.

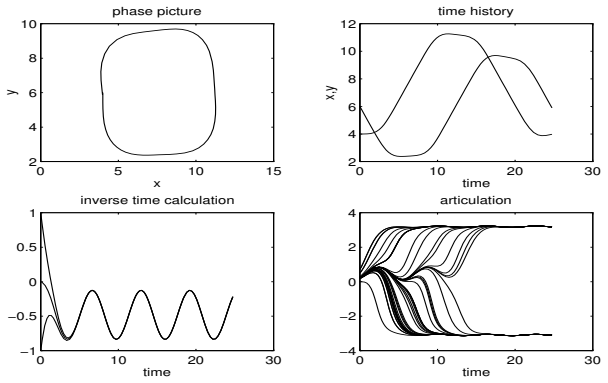

Figure 2: *Backward motion*

The case $p = \text{const}$ corresponds to a desired path of circular shape or straight lines and was analyzed in (l. Bushnell *et al.*, 1994). The Riccati equation has constant coefficients and can be analytically solved using reduction to the linear system. For industrial application both assumptions of small ε and slowly varying p usually hold.

For $\varepsilon = 0$ and $p = \text{const}$ two stationary solutions are $\varphi_1^0 = 2\ \arctan(p), \quad \varphi_2^0 = \pi$. Using small parameter approximation, two solutions engendered by φ_1^0 and φ_2^0 can be found as follows

$$\varphi_1^0 = 2\ \arctan(p(1 + \varepsilon\frac{1+2p^2}{2})),$$

$$\varphi_2^0 = 2\ \arctan(\frac{2}{p\varepsilon} - \varepsilon\frac{p(1+p^2)}{2})$$

In the general case Riccati equation could be reduced to the second order system of linear differential equations. Essential property consists in the existence of two solutions, one of which is always stable, but another one unstable.

Unstable solutions can be made stable by reversing the time and the direction of motion (sign(V_M)). Thus equations (1)–(4) can be used to obtain the desired articulation angle along the backward maneuver. Using (1) and (2) to compute ψ, the *generalized input* can be subsequently determined from (3), and then (4) is used for stable computations of an articulation angle φ. Figure 2 illustrates the backward maneuver of following a path consisting of successively executed turns and straight line parts (left top plot). This is an example of essentially non-stationary path. Direct calculations of the articulation angle give an "unnatural" stable solution closed to π for slightly asymmetrical machine (right bottom plot). If this solution is used for control, the vehicle will fold up instead of following the required path. The time inversion allows to obtain the correct result via numerically stable calculations (left bottom plot).

The results discussed above are closely related to the behavior of a trailers convoy pulled by a car. (l. Bushnell *et al.*, 1994). The description of the motion as using the Riccati equation generalizes those of (l. Bushnell *et al.*, 1994) where only circular and straight line trajectories where considered. On the other hand, our results are motivated by the "controlled joint" scheme, in such a case the "unstable behavior" has to be taken into account, the articulation angle along the path (including backward maneuvers) has to be calculated and subsequently used by an appropriate path tracking controller.

4. MODELING OF A TRACKED VEHICLE

A vehicle model with three degrees of freedom is adopted (Ahmadi *et al.*, 2000). The vehicle is supposed to undergo a motion in the horizontal plane, that is usually the case for a drilling rig in open pit mines–the targeted application of our research The traction and longitudinal resistance forces, as well as the distributed lateral friction forces are included in modeling. Most of existing models have some intrinsic limitations, *e.g.*, only forward maneuvers are considered or only circular and straight line paths are allowed, etc. A more complete model, capable of simulating a large variety of maneuvers of the vehicle is presented here.

The following assumptions and notations are used: the weight of the vehicle is equally divided on both tracks; (X, Y, ψ) represent the coordinates of the center of gravity (point M) in the fixed frame and the vehicle heading. A second coordinate system Mxy is attached to the vehicle with its Mx-axis coinciding to forward looking longitudinal axe of the vehicle, and My-axis being left orthogonal to Mx. The desired path P is defined by the smooth curve $(X(s)Y(s))$ in global coordinates with the radii of curvature $R(s)$ at each point; the vehicle moves with the velocity $\bar{V}$. Figure 3 illustrates the force distribution: F_l, R_l, F_r, R_r are the traction and resistance forces exerted to the vehicle through the left and right tracks respectively.

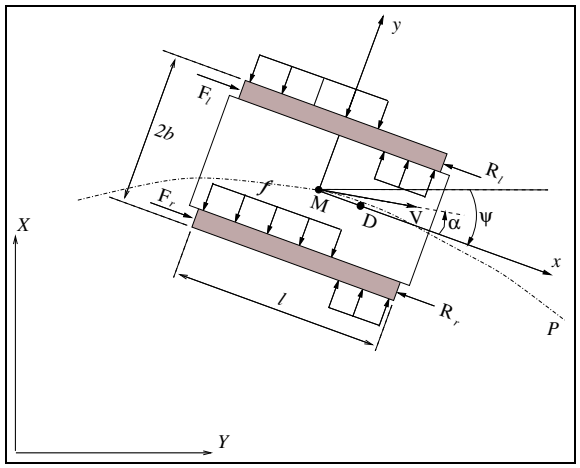

Figure 3: *Tracked vehicle's force model.*

We denote by v the signed desired velocity of the vehicle (positive if the forward motion is required and negative for a backward motion), and by α an angle between the direction of motion $v\bar{V}$ and Mx. It should be emphasized that the direction of backward motion is opposite to the $\bar{V}$, and due to the vehicle skidding, its direction is not tangent to the path. As a result, the angular speed $\dot{\psi}$ is not equal to

the rotation rate of the velocity vector $\omega = \mid v \mid /R$. For the same reason, the instantaneous center of rotation does not coincide with the center of the path curvature and the corresponding radii are different. In this modeling, the location of the vanishing point D of the lateral speed defined by

$$MD = \tilde{d} = \dot{y}/\dot{\psi} = -v \sin\alpha/\dot{\psi}, \tag{8}$$

is very important and will be used later.
Basic equations of motion in x–y coordinates, (see (Shiller *et al.*, 1994; Ahmadi *et al.*, 2000)), are as follows:

$$\begin{aligned} m\ddot{x} &= (F_l + F_r - R_l - R_r) \\ m\ddot{y} &= 4fd \\ I\ddot{\psi} &= (F_l - R_r)b - (F_i - R_i)b - 2f(\frac{l^2}{4} - d^2), \end{aligned} \tag{9}$$

where m is the mass of the vehicle, F and d are introduced below.

Under assumption of the uniform distribution of the weight along the track, the shear force density f is proportional to the pressure per unit of the track length $w = mg/2l$:

$$f = \mu\, w = \mu\, m\, g/(2l)$$

To compute the lateral forces, we introduce the saturation function $SAT(x, x_-, x_+) = max\{x_-, min\{x, x_+\}\}$ and denote:

$$d = SAT(\tilde{d}, -l/2, l/2) \tag{10}$$

Then we obtain using Figure 3:

$$F_{lat} = 4\, sign(v\,\omega)\, f\, d \tag{11}$$

The traction forces F_l and F_r are related to the left and right track slips i_l and i_r via the commonly used exponential expression (Bekker, 1969)

$$F_{tr} = F_{max}\left[1 - \frac{\nu}{|i|}\left(1 - e^{-|i|/\nu}\right)\right] \cdot \text{sign}(i), \tag{12}$$

where $\nu = k/l$, $F_{max} = S\,\tau$, S - is the track area, and τ and k are the soil parameters (Bekker, 1969).

The left and right track slips are defined as

$$\begin{aligned} i_l &= V_l/(r\omega_l) \qquad & V_l &= \dot{x} - b\dot{\psi} - r\omega_l \\ i_r &= V_r/(r\omega_r); \qquad & V_r &= \dot{x} + b\dot{\psi} - r\omega_r \end{aligned}$$

where r and ω_l, ω_r are the radius and the angular velocities of the sprockets, and V_l and V_r are the slip velocities for each track.

Detailed description of the modeling in (Ahmadi *et al.*, 2000) and is not included for the sake of brevity. We focus here on the computational aspects of the orientation planning for tracked vehicles.

5. NONHOLONOMIC PLANNING FOR TRACKED VEHICLES

Trajectory planning for conventional vehicles consists of two separate procedures, namely: velocity planning (or scheduling) and path planning. Due to the inevitable slippage of tracks and the dependence of traction forces on track slippage, those two problems cannot be solved separately. The scheduling problem and the shape definition have to be solved first. Then the orientation of the vehicle along the path can be calculated. The path $(X(s),\, Y(s))$ is supposed to be known as well as the linear speeds $v(s)$ along the path as it is described above. For a targeted application this is a natural assumption as a drill rig is usually required to move along the prescribed path at the constant speed between two pre-specified locations and its acceleration/deceleration can be easily accounted for.

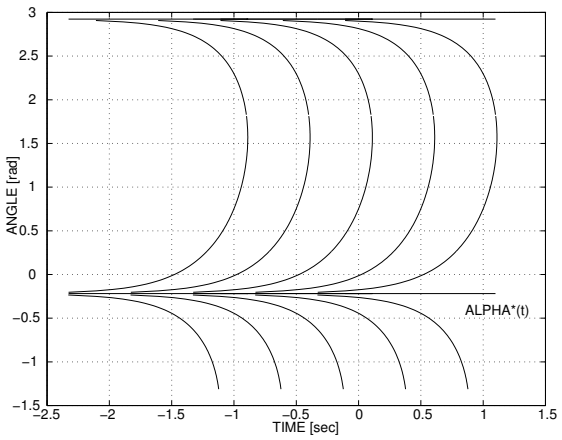

Figure 4: *Structure of solutions*

In order to take the slippage into account, let us evaluate the balance of forces in the lateral direction My. From (1)-(4) we obtain:

$$\begin{aligned} sign(v\,\omega)\,\frac{2\,\mu\,g}{l}\,SAT(-\frac{v\,sin\alpha}{\dot{\psi}}, -l/2, l/2) = \\ = v\,\omega\,\cos\alpha + \dot{v}\,\sin\alpha \end{aligned} \tag{13}$$

Using the relationship between $\dot{\alpha}$, $\dot{\psi}$, and ω:

$$\dot{\alpha} + \dot{\psi} = \omega, \tag{14}$$

and introducing the "natural frequency" C:

$$C = \sqrt{2\,\mu\,g/l}, \tag{15}$$

the equation (13) can be rewritten in terms of α for "before-saturation" case ($\tilde{d} = d$) as

$$\dot{\alpha} = \omega + \frac{C^2 sign\omega\, v\,\sin\alpha}{\omega v\,\cos\alpha + \dot{v}\,\sin\alpha} \tag{16}$$

To illustrate the use of this equation, one can calculate the stationary solution of (16) for the case when $\dot{v} = 0$. For $\dot{\alpha} = 0$ we get $C^2 \tan\alpha = -\omega \mid \omega \mid$, hence

$$\alpha^* = -atan(\omega \mid \omega \mid /C^2). \tag{17}$$

This is a purely analytical result that cannot be obtained as a numerical solution of (16)due to numerical instability. Namely, equation(9) has a closed form solution of the form

$$t = \Phi(\tan\alpha), \text{ where} \tag{18}$$

$$\Phi(z) = \frac{C^2 \mid \omega \mid}{\omega^4 + C^4}\left(\frac{\omega \mid \omega \mid}{C^2}\arctan z + \ln\frac{C^2 z + \omega \mid \omega \mid}{C^2\sqrt{z^2+1}}\right.$$

The global structure of solutions in the $(t,\ \alpha)$-plane is illustrated in Figure 4.

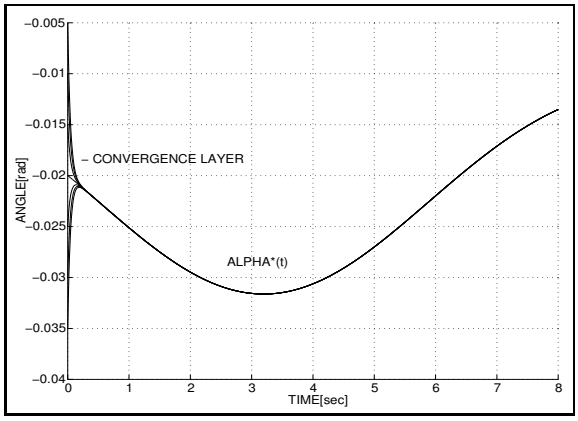

Figure 5: *Time-varying balanced solution*

The stationary solution (10) is a unique (up to the periodicity over α) solution that can be extended to the unbounded time domain, we will call it "balanced solution". All other solutions as illustrated in figure (3) diverge from the balanced solution and escape to infinity (in $\dot{\alpha}$) in finite time. Therefore any direct numerical solution of (9) diverges from the balanced solution (10) and cannot be used to compute the balanced solution.

For the time invariant case, this numerical instability seems not to be very important since the balanced solution is known. For the time-varying case, an analytical solution may not exist, which makes impossible the direct computation of the "balanced" type solutions in the presence of such instabilities. By thoroughly analyzing the time-varying "before-saturation" case, we have demonstrated that the solutions of (16) still has the similar structure. We have shown that under some technical assumptions there exist a unique balanced-type solution. It is repulsive in the direct time, but it is attractive in the inverse time and can be obtained by backward integration from almost any terminal conditions.

Namely, if we fix the terminal time T and introduce $\tau = T - t$, and consider two solutions, $\alpha^+(\tau)$ and $\alpha^-(\tau)$ starting from α_0^+, α_0^- at $\tau = 0$, their difference $z = \alpha^+(\tau) - \alpha^-(\tau)$ decays monotonically to zero with an explicit upper bound. The demonstration is rather involved and is not presented here.

Due to that monotonicity, all solutions converge to a unique limiting solution - balanced solution, which is de-

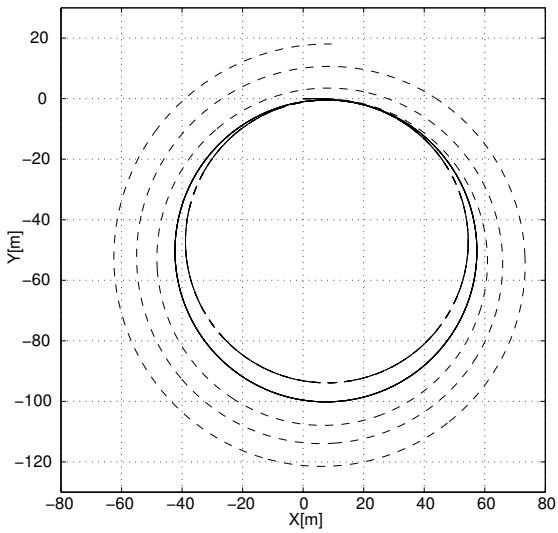

Figure 6: *Circular path execution*

noted below by $\alpha^*(\tau)$. Once this solution is computed, we inverse the time again $t = T - \tau$ and use $\alpha^*(t)$ as the desired value of the "skidding angle" along the path. Figure 5 illustrates the results of the proposed computational method when ω and v vary in time ($0.15sec^{-1} \leq -\omega(t) \leq 0.25sec^{-1};\ 5m/sec \leq v \leq 15m/sec$). All solutions converge very fast to the balanced solution $\alpha^*(t)$, which can not be found nor analytically neither by the direct numerical integration.

In the above discussion we have limited ourselves by the non-saturated case $\tilde{d} = d$. To include the saturation effects,

$$\mid \frac{v\ \sin\alpha*}{\omega - \dot{\alpha}} \mid \leq \frac{l}{2} \tag{19}$$

has to be verified for the balanced solution.

E.g. for the following parameters $l = 5m, v = 10m/s, R = -50m, \mu = 0.19$, the balanced solution is $\alpha^* = 0.1$ and it does not satisfy to (12). As a result, the stationary turn with these parameters will not occur. If the the value of μ increases up to 0.5, we get $\alpha^* = 0.02$, satisfying to (12). In general, the following condition guarantees that the balanced solution α^* is acceptable.

$$\mid \omega \mid \geq \frac{2 \mid v \sin\alpha^* \mid}{l} \tag{20}$$

Under an assumption that $l/(2 \mid R \mid)$ is small (the length of the track with respect to the diameter of turn) we may rewrite (13) as

$$\mu g R \geq v^2 \tag{21}$$

We have found this condition very important for planning the maneuver of tracked vehicles, *i.e.*, when turning at a given radius R, higher speeds are allowed on a terrain with higher coefficient of the lateral resistance. For the given speed there is a lower bound for the allowable radius given a particular value of μ. And *vice versa*, there is a lower bound for μ if the maneuver with a particular R is required.

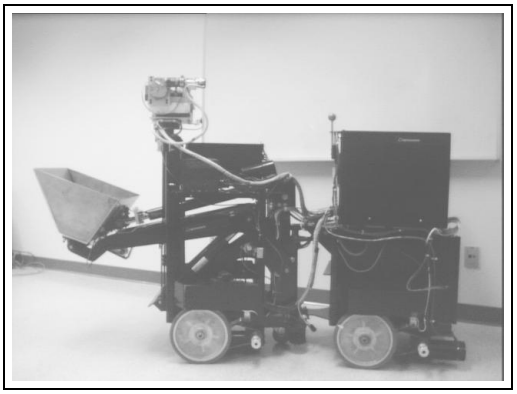

A. Articulated vehicle: mini-LHD

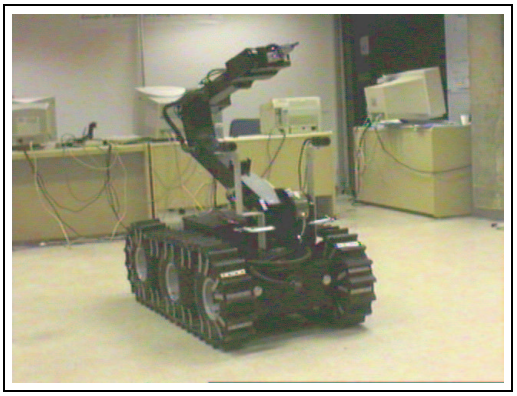

B. Tracked vehicle: MR5

Figure 7: *Experimental vehicles*

Figure 6 illustrates the execution of a turn at $R = -50m$ with required speed $v = 10m/sec$ on a terrain with $\mu = 0.19$ ("-" corresponds to an' anti-clockwise turn). Condition (21) is not met, hence, for the execution of this maneuver the desired speed was reduced to 9.4 m/sec that corresponds to the boundary of (21). Then the control inputs corresponding to this motion are calculated and the open loop run is executed. The system follows exactly the required circular path (Figure 6). If $v = 10m/sec$ is conserved and corresponding $\alpha = \alpha_1^*$ is used, the smaller circle ($R = 46m$ is realized. If the condition (21) is not taken into account at all and $\alpha = \alpha_2^*$ is used, the spiral-shape trajectory with fast growing α is observed (figure 6).

6. IMPLEMENTATION ISSUES

The described approach to the articulated and skid-steering vehicle guidance has been implemented on the laboratory size platforms mini-LHD and MR5 illustrated in figures 7 (A) and 7 (B) respectively. On-board control algorithms for path-following utilize feed-forward terms based on off-line computations of articulation and heading described above. Ongoing projects address outdoor testing in more realistic environments and implementation on real mining equipment.

7. CONCLUSIONS

An enhanced path-planning methodology for articulated and skid-steering vehicles is described in this paper. Additional parameters specifying vehicle heading, namely articulation and skidding angles are computed along the planning phase. and used for constructing feed-forward terms along the execution phase. Proposed methodology is of particular importance for the paths with a varying curvature and backward maneuvers. Using computations in backward time, our proposed procedure overcomes the numerical instability reported in (l. Bushnell *et al.*, 1994) for articulated vehicles and in (Shiller *et al.*, 1994) for skid steering vehicles.

By incorporating our enhanced planning procedure into the control loop we make the orientation error decaying faster and also improve the overall controller performance. This procedure constitutes the low cost improvements since no additional sensing capabilities or more actuators are needed but only some additional off-line processing and complementary feed-forward terms in controllers.

ACKNOWLEDGMENTS

The financial support of the NSERC Industrial Chair in Mining Automation is gratefully acknowledged.

References

Ahmadi, M., V. Polotski and R. Hurteau (2000). Path tracking control of tracked vehicles. In: *IEEE Int. Conf. on Robotic and Automation*. Los Angeles, CA. pp. 27–35.

Bekker, M. G. (1969). *Introduction to Terrain-Vehicle Systems*. University of Michigan Press. Ann Arbor.

DeSantis, R. (1997). Modeling and path-tracking for a load-haul-dump mining vehicle. *ASME J. Dynamic Systems, Measurement and Control* pp. 342–349.

Kamke, E. (19833). *'DifferentialGleichungenk*. Wiley.. Stuttgart.

l. Bushnell, B. Mirtich, A. Sahai and M. Secor (1994). Off tracking bounds for a car pulling trailers with kingpin hitching. In: *Int. Conf. on Decision and Control*.

Peck, J. and P. Hendrics (1997). Gps-based navigation systems on mobile mining equipment for open-pit mine. *CIM Bulletin* pp. 114–119.

Polotski, V. (2000). New reference point for guiding an articulated vehicle. In: *Int. Conf. on Control Applications*.

Polotski, V., J. N. Bakambu, W. Wu and P. Cohen (2000). Navigation system for underground mining vehicles: Architecture and experimental setup. In: *31st Int. Symp. on Robotics*.

Shiller, Z., M. Serate and M. Hua (1994). Trajectory planning of tracked vehicles. In: *IEEE Int.Conf. on Robotic and Automation*.